

Numerical cubature and hyperinterpolation over Spherical Polygons *

A. Sommariva
University of Padova, Italy

March 9, 2024

Abstract

The purpose of this work is to introduce a strategy for determining the nodes and weights of a low-cardinality positive cubature formula nearly exact for polynomials of a given degree over spherical polygons. In the numerical section we report the results about numerical cubature over a spherical polygon \mathcal{P} approximating Australia and reconstruction of functions over such \mathcal{P} , also affected by perturbations, via hyperinterpolation and some of its variants. The open-source Matlab software used in the numerical tests is available at the author's homepage.

2010 AMS subject classification: Primary 41A10, 42A10, 65D05, 65D32.

Keywords: Algebraic cubature, spherical triangles, spherical polygons, hyperinterpolation.

1 Introduction

In [20] the authors introduced a numerical code for the computation of cubature formula on spherical triangles of the unit-sphere \mathbb{S}_2 , nearly exact for polynomials $p_n \in \mathbb{P}_n(\mathbb{S}_2)$, i.e. numerically achieving a given total polynomial degree n . The algorithm was based on subperiodic trigonometric gaussian quadrature for planar elliptical sectors and on Caratheodory-Tchakaloff quadrature compression via NNLS. The final rule had internal nodes, positive weights and cardinality at most equal to $(n+1)^2$, that is the dimension of the vector space $\mathbb{P}_n(\mathbb{S}_2)$.

Later in [21], they move their attention to the computation of an orthogonal polynomial basis on spherical triangles, via the formula described above, and to the construction of the corresponding weighted orthogonal projection (hyperinterpolation) of a function sampled at the cubature nodes.

*Work partially supported by the DOR funds of the University of Padova, and by the INdAM-GNCS grant *Kernel and polynomial methods for approximation and integration: theory and software for applications*. This research has been accomplished within the RITA *Research Italian network on Approximation*, the SIMAI Activity Group ANA&A and the UMI Group TAA *Approximation Theory and Applications*.

¹Corresponding author: alvise@math.unipd.it

Having in mind the studies of real world problems, e.g. coming from geo-mathematics, we move here to the more general setting of spherical polygons \mathcal{P} of \mathbb{S}_2 .

We first show how to implement such a cubature rule nearly exact for polynomials in $\mathbb{P}_n(\mathbb{S}_2)$, with internal nodes, positive weights and cardinality at most equal to $(n+1)^2$. Next we investigate its qualities when applied to certain spherical polygons, reporting cardinalities, cputimes as well as cubature errors relatively to certain integrands with different regularity.

Later we give a brief introduction to the classical hyperinterpolation and to some of its variants useful in case of noisy data, finally testing the numerical reconstruction of functions also in the case of perturbations given by impulsive and gaussian noise.

2 Numerical cubature on spherical polygons

We start our study introducing some definitions that are useful in the paper.

A *great circle* is the intersection of the unit-sphere $\mathbb{S}^2 = \{(x, y, z) : x^2 + y^2 + z^2 = 1\}$ with a plane passing through the origin.

Let V_1, \dots, V_L be distinct points of \mathbb{S}^2 and set $V_0 = V_L$. A *spherical polygon* with vertices $\{V_k\}_{k=1, \dots, L}$ is the region $\mathcal{P} \subset \mathbb{S}^2$ whose boundary $\delta\mathcal{P}$ is determined by the geodesic arcs $\{\gamma_k\}_{k=0, \dots, L}$, where each edge γ_k is the portion of the great circle joining V_k with V_{k+1} , and is oriented counterclockwise.

In this paper we suppose that the spherical polygon \mathcal{P} is contained in a cap whose *polar angle* is strictly inferior than π . We notice that, for the purpose of determining a cubature rule over \mathcal{P} , if the spherical polygon has not this feature then it can always be subdivided in spherical polygonal regions \mathcal{P}_k , each one contained in a cap whose *polar angle* is strictly inferior than π , whose interior do not overlap and whose union is \mathcal{P} . Next, one can apply the procedure that we will explain below on each \mathcal{P}_k , obtaining a *composite* rule on \mathcal{P} .

In this section we show how to obtain a cubature rule of PI-type over such a spherical polygon \mathcal{P} , i.e. a formula that has *positive weights* $\{w_k\}_{k=1, \dots, M}$ and *internal nodes* $\{Q_k\}_{k=1, \dots, M}$, and that is nearly exact in the space $\mathbb{P}_n(\mathbb{S}_2)$ of polynomials on \mathbb{S}_2 of total degree at most n .

It can be proven that if $\mathcal{P} \subset \mathbb{S}_2$ is a spherical polygon, each of whose edges have length strictly less than π , and \mathcal{P} does not contain a great circle, then \mathcal{P} has a spherical triangulation [13]. Consequently, since \mathcal{P} is contained in a cap whose *polar angle* is strictly inferior than π , we can conclude that there is a spherical triangulation of \mathcal{P} .

The latter can be obtained as follows:

1. denoting by $C_{\mathcal{P}}$ the centroid of \mathcal{P} , we determine the *gnomonic projection* $\tilde{\mathcal{P}}$ of \mathcal{P} on the plane $\pi_{C_{\mathcal{P}}}$ tangent in $C_{\mathcal{P}}$ to the unit-sphere;
2. compute a triangulation over the planar polygon $\tilde{\mathcal{P}}$ (e.g. by Matlab built-in environment `polyshape` that determines a minimal triangulation), i.e. $\tilde{\mathcal{P}} = \cup_{i=1}^m \tilde{\mathcal{T}}_i$ where $\tilde{\mathcal{T}}_i \subset \pi_{C_{\mathcal{P}}}$ are planar triangles whose interiors do not overlap, i.e. if $j \neq k$ then $\text{int}(\tilde{\mathcal{T}}_j) \cap \text{int}(\tilde{\mathcal{T}}_k) = \emptyset$;

3. *map back to the sphere*, by means of the inverse of the gnomonic projection, each planar triangle $\tilde{\mathcal{T}}_k$ into a spherical triangle \mathcal{T}_k , obtaining the required spherical triangulation.

Since $\{\mathcal{T}_k\}_{k=1,\dots,m}$ is a spherical triangulation of \mathcal{P} , if we determine a cubature rule of PI-type with ADE equal to n over each spherical triangle \mathcal{T}_k then by the addivity of integration we have immediatly a rule with the same features also on \mathcal{P} .

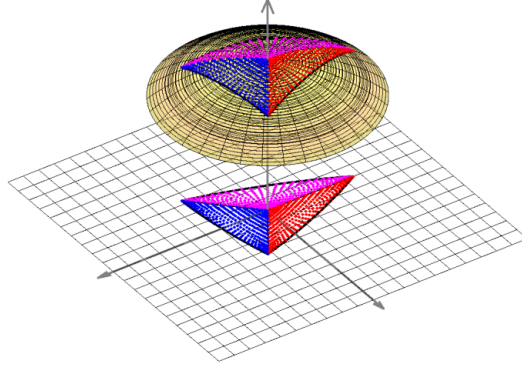


Figure 1: cubature nodes (and weights) on a spherical triangle lifted from the projected elliptical triangle.

For this reason, we concentrate our efforts in determining a rule over a spherical triangle \mathcal{T} contained in a cap whose *polar angle* is strictly inferior than π . To this purpose, we recall the technique that the authors have used in [20].

With no loss of generality, up to a suitable rotation, we can suppose that the spherical triangle $\mathcal{T} = ABC$ has the centroid $C_{\mathcal{T}} = (A + B + C) / \|A + B + C\|_2$ coinciding with the North Pole $(0, 0, 1)$ and furthermore is strictly contained in the northern-hemisphere, i.e. it does not contain any point of the equator.

Then, if $f \in C(\mathcal{T})$, $g(x, y) = \sqrt{1 - x^2 - y^2}$,

$$I_{\mathcal{T}} := \int_{\mathcal{T}} f(x, y, z) d\sigma = \int_{\mathcal{T}^{\perp}} f(x, y, g(x, y)) \frac{1}{g(x, y)} dx dy,$$

where \mathcal{T}^{\perp} is the projection of \mathcal{T} onto the xy -plane, that is the curvilinear triangle whose vertices, say $\hat{A}, \hat{B}, \hat{C}$, are the xy -coordinates of A, B, C , respectively (see Figure 1).

The sides of \mathcal{T}^{\perp} are arcs of ellipses centered at the origin, being the projections of great circle arcs. Then we can split the planar integral into the sum of the integrals on three elliptical sectors \mathcal{S}_i with $i = 1, 2, 3$, obtained by joining the origin with the vertices $\hat{A}, \hat{B}, \hat{C}$, namely

$$I_{\mathcal{T}} = \int_{\mathcal{T}^{\perp}} f(x, y, g(x, y)) \frac{1}{g(x, y)} dx dy = \sum_{i=1}^3 \int_{\mathcal{S}_i} f(x, y, g(x, y)) \frac{1}{g(x, y)} dx dy$$

If the purpose is to compute an algebraic rule over \mathcal{T} , with algebraic degree of exactness $ADE = n$, positive weights and internal nodes (i.e. rules of PI-type) we face the problem that while f is a polynomial of total degree n then being $g(x, y) = \sqrt{1 - x^2 - y^2}$, we have that in general $f(x, y, g(x, y)) \frac{1}{g(x, y)}$ may not be a polynomial.

To see this properly, let

- $f(x, y, z) = x^\alpha y^\beta z^\gamma$, $0 \leq \alpha + \beta + \gamma \leq n$, $\alpha, \beta, \gamma \in \mathbb{N}$;
- $g(x, y) = \sqrt{1 - x^2 - y^2}$.

Thus

$$f(x, y, g(x, y)) \frac{1}{g(x, y)} = x^\alpha y^\beta (1 - x^2 - y^2)^{(\gamma-1)/2}.$$

In particular, if γ is

- *odd* then $f(x, y, g(x, y)) \frac{1}{g(x, y)}$ is a *polynomial* of degree at most n ,
- *even* then $f(x, y, g(x, y)) \frac{1}{g(x, y)}$ is $1/g$ multiplied for a *polynomial* of degree at most n .

To overcome this problem, having in mind to produce a formula that is numerically exact over bivariate polynomials of a certain total degree, we proceed as follows.

First, we approximate $1/g$ by a polynomial p_ε of degree $m = m_\varepsilon$ such that $|p_\varepsilon - 1/g| \leq \varepsilon \cdot 1/|g|$. Next, since $f/g \approx f \cdot p_\varepsilon \in \mathbb{P}_{n+m}$, we integrate $f \cdot p_\varepsilon$ instead of f/g on the elliptical sectors \mathcal{S}_i , $i = 1, 2, 3$.

Finally, as observed before, determining a rule of algebraic degree of exactness $n+m$ over each elliptical sector \mathcal{S}_i , $i = 1, 2, 3$, with internal nodes, and positive weights then we have a rule on $\mathcal{T}^\perp := \cup_{i=1}^3 \mathcal{S}_i$ with nodes $(x_k, y_k)_{k=1, \dots, M}$, weights $w_{k=1, \dots, M}$ of PI-type.

Mapping back the nodes on the sphere, we have a rule over the spherical triangle that is near algebraic with ADE n since

$$\int_{\mathcal{T}} f(x, y, z) d\sigma \approx \sum_{j=1}^M \frac{w_j}{\sqrt{1 - x_j^2 - y_j^2}} f(x_j, y_j, \sqrt{1 - x_j^2 - y_j^2}). \quad (1)$$

At this point, there are some aspects of this procedure that require some further explanation (for details, see also [20]).

About the computation of a cubature formula with prescribed degree of exactness over each elliptical sector \mathcal{S}_i , since each \mathcal{S}_i is an affine transformation of a circular sector \mathcal{S}_i^* of the unit-disk, it is sufficient to obtain a formula on \mathcal{S}_i^* as described in [9] and map it to \mathcal{S}_i (some care on the weights that must be multiplied by absolute value of the transformation matrix determinant).

Another issue is the computation of $m = m_\varepsilon$. To this purpose, setting $\varepsilon = 10^{-15}$, it turns out that it is sufficient to find what is a (small) degree m_ε for which there exist $p_{m_\varepsilon} \in \mathbb{P}_{m_\varepsilon}$ that approximates $1/\sqrt{1-t}$ where $t \in [0, \max\{\|\hat{A}\|_2^2, \|\hat{B}\|_2^2, \|\hat{C}\|_2^2\}]$, with a relative error at most ε in ∞ -norm. Such $m = m_\varepsilon$ can be quickly estimated by Chebfun [7] and stored in tables.

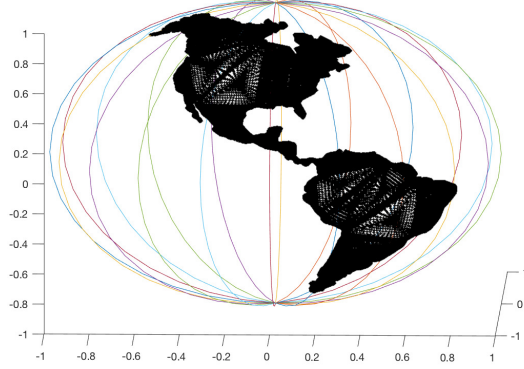


Figure 2: The 380544 nodes of a rule of PI-type with ADE=8, on a spherical polygon approximating South and North America, before Caratheodory-Tchakaloff compression. The computation of this formula requires about 10 seconds.

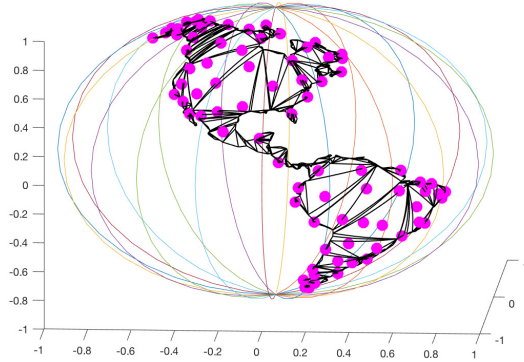


Figure 3: Triangulation of a spherical polygon (967 spherical triangles) and cubature rule of PI-type with ADE=8, 81 points, after Caratheodory-Tchakaloff compression (magenta). The compression cptime requires approximately 3.5 seconds.

We end this section by recalling some basics on the Caratheodory-Tchakaloff rule compression. From the nodes $\{P_k\}_{k=1,\dots,M}$ and weights $\{w_k\}_{k=1,\dots,M}$ of the PI-type rule on \mathcal{P} , with $M \geq (n+1)^2$, we can extract one with the same features but with cardinality at most $(n+1)^2$, see [18]. This is guaranteed by Tchakaloff theorem on positive cubature, that in the framework of discrete measures can be demonstrated via the Caratheodory theorem on conical linear combinations of finite-dimensional vectors (applied to the columns of the Vandermonde-like matrix of a moment matching system)

and one of these solutions can be obtained numerically by means of Lawson-Hanson algorithm [11]. We observe that there are several Matlab implementations of the latter procedure, as the Matlab built-in routine `lsqnonneg` or that proposed by Slawski in [14]. A new recent fast variant has been introduced in [8], and view of its performance, we will use it in our cubature routines to obtain one of these so called *Caratheodory-Tchakaloff* formula.

In order to show our approach to a real world problem, in Figure 2, we consider the spherical polygon \mathcal{P} that is an approximation of South and North America (without considering minor islands, rivers and lakes), we plot the 380544 cubature rule nodes of a formula with a numerical ADE equal to 8, and then in Figure 3 we exhibit the spherical triangulation and the extracted Caratheodory-Tchakaloff rule with 81 points (exactly the dimension of the polynomial space of total degree 8 on \mathbb{S}_2) and again numerical ADE equal to 8.

2.1 Numerical experiments

We have implemented the procedure described above in Matlab, so determining the nodes and the weights of a cubature rule over the spherical polygon \mathcal{P} that approximately integrates all the polynomials $p \in \mathbb{P}_n^3(\mathbb{S}_2)$, for a fixed $n \in \mathbb{N}$. The codes are freely available at [17].

A first problem is that there is no known way to achieve $I_{\mathcal{P}}(f) = \int_{\mathcal{P}} f(x, y, z) d\sigma$, when \mathcal{P} has such a complicate geometry. To overcome this problem we have also implemented a basic adaptive code, that computes $I_{\mathcal{P}}(f)$ with a relative error of 10^{-14} .

As region, we consider Australia (without Tasmania as well as minor islands), whose boundary is provided by the Matlab Mapping toolbox, via longitude-latitude coordinates. Though our software can manage domains that are not simply connected, we did not consider, for sake of simplicity, lakes and rivers. This complex spherical polygon consists of 169 vertices and is the union of 167 spherical triangles whose interiors do not overlap.

Though the Earth radius is not unitary, in our battery of tests we suppose that $\mathcal{P} \subset \mathbb{S}_2$. We observe that it is not restrictive, since an integral on a sphere of radius r can be easily reformulated as one on \mathbb{S}_2 .

As for the integrands, setting $(x_0, y_0, z_0) \approx (-0.6325, 0.6668, -0.3908) \in \mathbb{S}_2$ as an approximation of australian centroid, and

$$h(x, y, z) = (x - x_0)^2 + (y - y_0)^2 + (z - z_0)^2$$

we consider the test functions

1. $f_1(x, y, z) = 1 + x + y^2 + x^2 y + x^4 + y^5 + x^2 y^2 z^2$, i.e. a polynomial, of total degree 6;
2. $f_2(x, y, z) = \cos(10 \cdot (x + y + z))$, a function with some oscillations;
3. $f_3(x, y, z) = \sin(-h(x, y, z))$, i.e. an analytic function;
4. $f_4(x, y, z) = \exp(-h(x, y, z))$, i.e. an analytic function;

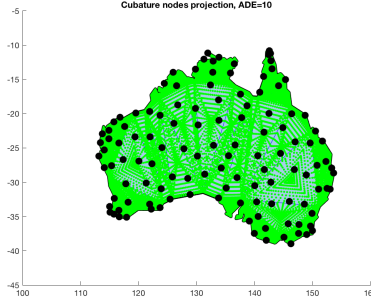


Figure 4: cubature nodes of a formula of PI-type having ADE equal to 10, on a coarse approximation of Australia using 169 points of \mathbb{S}_2 . To this purpose, we determine a triangulation of such a spherical polygon in 167 spherical triangles, obtained a first rule of PI-type with 82413 nodes, and then a compressed one with 121, with moments error of $\approx 5 \cdot 10^{-15}$. The computation of the Caratheodory-Tchakaloff formula took takes 6 seconds.

5. $f_5(x, y, z) = ((x - x_0)^2 + (y - y_0)^2 + (z - z_0)^2)^{3/2}$, i.e. a $C^1(\mathcal{P})$ function;
6. $f_6(x, y, z) = ((x - x_0)^2 + (y - y_0)^2 + (z - z_0)^2)^{5/2}$, i.e. a $C^2(\mathcal{P})$ function.

Due to their properties, we expect that the integration of f_2 , f_5 and f_6 by (numerically) algebraic rules will provide *inferior* results w.r.t. f_1 , f_3 and f_4 . Furthermore, $I_{\mathcal{P}}(f_1)$ will be approximated with a relative error for formulas with degree of exactness at least 6 of about 10^{-14} or less. The numerical results of this battery of tests are described in Figure 5, and as expected the better results are obtained by f_1 , f_3 and f_4 while the convergence is slower for f_2 , f_5 and f_6 .

Finally, in Table 1, we have listed the cardinalities of the rules before and after the Caratheodory-Tchakaloff compression, their ratios, and the cputime required by the numerical procedure to determine the Caratheodory-Tchakaloff rule.

These tests show that the rule compression is remarkable and that for mild ADE the cputime necessary to produce a formula of PI type with low cardinality is acceptable, especially in view of the complicated geometry of the integration domain.

All our tests have been performed on a 2.7 GHz Intel Core i5 with 16 GB of RAM, using Matlab 2022a, in which is available the `polyshape` environment.

3 Hyperinterpolation on spherical polygons

Hyperinterpolation has been introduced in the seminal paper by I.H. Sloan in 1995 (see [15]), in the framework of approximation of multivariate functions, and is essentially equivalent to a truncated Fourier expansion in a series of orthogonal polynomials for some discrete or continuous measure.

From then, many aspects has been deepened, either theoretically either from the implementative point of view, proposing hyperinterpolation as a valuable alternative to

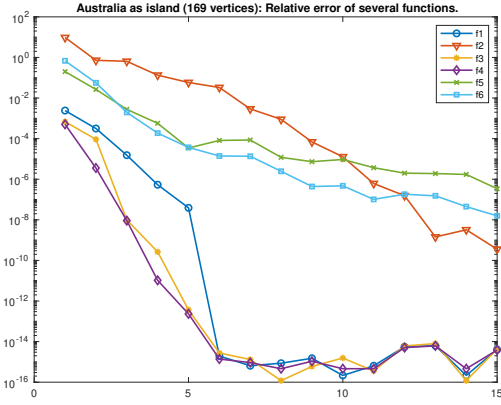


Figure 5: cubature relative errors, in semilogarithmic scale, obtained by approximating $I_{\mathcal{D}}(f_k)$, for $k = 1, 2, \dots, 6$, by rules with ADE equal to $1, 2, \dots, 16$.

n	# basic	# comp	Cratio	CPU	n	# basic	# comp	Cratio	CPU
1	20613	4	5153:1	0.6s	9	72441	100	724:1	3.9s
2	25965	9	2885:1	0.6s	10	82413	121	681:1	6.1s
3	30564	16	1910:1	0.7s	11	90408	144	627:1	14s
4	37071	25	1482:1	0.8s	12	101535	169	600:1	17s
5	42519	36	1181:1	1.1s	13	110379	196	563:1	22s
6	50181	49	1024:1	1.3s	14	122661	225	545:1	33s
7	56478	64	882:1	1.8s	15	132354	256	517:1	48s
8	65295	81	806:1	2.6s	16	145791	289	504:1	62s

Table 1: Cardinalities of the rule before and after the compression, respectively #basic and #comp, compression ratio Cratio and CPU time in seconds.

interpolation, without the issue of determining for the latter a good set of points, e.g. with low Lebesgue constant. In particular, the application to many 2D and 3D domains has been explored, such as balls, cubes, unit sphere, but also less standard ones as polygons, circular sections [19], spherical rectangles [10] and spherical triangles [21].

Denoting by $\mathbb{P}_n^d(\Omega)$ the subspace of d -variate polynomials of total-degree not exceeding n , restricted to a compact set or manifold $\Omega \subset \mathbb{R}^d$ w.r.t. a given measure $d\mu$ on Ω , given

- an orthonormal basis of $\mathbb{P}_n^d(\Omega)$, say $\{p_j\}$, $1 \leq j \leq N_n = \dim(\mathbb{P}_n^d(\Omega))$,
- a cubature formula exact for $\mathbb{P}_{2n}^d(\Omega)$ with nodes $X = \{x_i\} \subset \Omega$ and positive weights $\mathbf{w} = \{w_i\}$, $1 \leq i \leq M$ with $M \geq N_n$,
- the scalar product $\langle f, g \rangle_M = \sum_{i=1, \dots, M} w_i f(x_i) g(x_i)$,

the hyperinterpolation of $f \in C(\Omega)$ is

$$(\mathcal{L}_n f)(x) = \sum_{j=1}^{N_n} \langle f, p_j \rangle_M p_j(x) = \sum_{i=1}^{N_n} w_i f(x_i) \sum_{j=1}^{N_n} p_j(x_i) p_j(x).$$

Applying this notion to our spherical setting, if $\Omega \equiv \mathcal{S}$ is spherical polygon strictly contained in a hemisphere, $d\mu = d\sigma$ is the surface measure on the sphere, then

1. by means of the routines in our Matlab package dCATCH, freely available at [22], we determine the required orthonormal basis $\{p_j\}$,
2. next we compute a cubature rule of degree $2n$ on Ω as previously shown,
3. finally we get the hyperinterpolant of degree n .

Items one and three require some explanation. Since the cubature formula with nodes $\{x_i\}_{i=1, \dots, M}$ and weights $\{w_i\}_{i=1, \dots, M}$ has ADE equal to $2n$, if $\{p_j\}_{j=1, \dots, N_n}$ is orthonormal w.r.t. this discrete measure, being exact for all the polynomials of total degree at most $2n$, it turns out that it is orthonormal also w.r.t. $d\sigma$. Next, denoting by $V_n \in \mathbb{R}^{M \times N_n}$ the Vandermonde matrix of the spherical harmonics basis $\{\phi_i\}_{i=1, \dots, N_n}$ evaluated at $\{x_i\}_{i=1, \dots, M}$, we first determine the QR factorization of $\sqrt{W}V_n$, i.e. a unitary matrix $Q \in \mathbb{R}^{M \times N_n}$ and an upper triangular one $R \in \mathbb{R}^{N_n \times N_n}$ such that $\sqrt{W}V_n = QR$ and then set

$$(p_1, \dots, p_{N_n}) = (\phi_1, \dots, \phi_{N_n})R^{-1}.$$

Since $U_n = V_n R^{-1} = (p_j(x_i))$ is the Vandermonde matrix w.r.t. the basis $\{p_k\}_{k=1, \dots, N_n}$, it can be easily checked that the latter is actually orthonormal w.r.t. the scalar product defined by the discrete measure generated by the cubature formula. Observe that R is non singular since V_n is full rank in view of the fact that the set $X = \{x_i\} \subset \Omega$ is $\mathbb{P}_n(\Omega)$ -determining.

Furthermore, the vector of hyperinterpolation coefficients $c^* = (c_j^*)_{j=1, \dots, N_n}$, such that $(\mathcal{L}_n f)(x) = \sum_{j=1}^{N_n} c_j^* p_j(x)$, that can be regarded as Fourier coefficients, can be conveniently computed in matrix form, being

$$c^* = U_n^T W f = (\sqrt{W}U_n)^T \sqrt{W}f = Q^T \sqrt{W}f, \quad f = (f(x_i))_{i=1, \dots, M}.$$

Concerning the quality of the approximation, there are many theoretical aspects that deserve to be cited, and in particular that if f is a continuous function in Ω then

$$\|f - \mathcal{L}_n f\|_{L^2(\Omega)} \leq 2\sqrt{\sigma(\Omega)} E_n(f, \Omega), \quad E_n(f, \Omega) = \min_{p \in \mathbb{P}_n(\Omega)} \|f - p\|_\infty, \quad (2)$$

so implying that if $p \in \mathbb{P}_n^d(\Omega)$ then $\mathcal{L}_n p = p$, as well as

$$\|f - \mathcal{L}_n\|_{L^\infty(\Omega)} \leq (1 + \|\mathcal{L}_n\|) E_n(f, \Omega) \quad (3)$$

where

$$\|\mathcal{L}_n\| = \sup_{f \neq 0} \frac{\|\mathcal{L}_n f\|_{L^\infty(\Omega)}}{\|f\|_{L^\infty(\Omega)}}.$$

For additional more technical details, see [19], [21].

Recently some hyperinterpolation variants have been studied, having in mind between various scopes also to improve the approximation quality in case of noisy data. We make a brief glance on some of them, as the filtered, Lasso and hybrid variants, useful later to comprehend the comparisons made in the numerical section.

In *filtered hyperinterpolation* [16], one introduces a *filter function* $h \in \mathcal{C}([0, +\infty))$ that satisfies

$$h(x) = \begin{cases} 1, & \text{for } x \in [0, 1/2], \\ 0, & \text{for } x \in [1, \infty). \end{cases}$$

It is straightforward to notice that depending on the behaviour in $[1/2, 1]$, one can define many filters, e.g. as used in [2]

$$h(x) = \begin{cases} 1, & x \in [0, \frac{1}{2}], \\ \sin^2(\pi x), & x \in [\frac{1}{2}, 1] \\ 0, & \text{for } x \in [1, \infty). \end{cases} \quad (4)$$

Denoting by $\lfloor \cdot \rfloor$ the floor function, by h the chosen *filter* and by $\langle f, g \rangle_M$ a discrete scalar product defined by an M -point cubature rule of PI-type in Ω with algebraic degree of exactness $L - 1 + \lfloor L/2 \rfloor$, the *filtered hyperinterpolant* $\mathcal{F}_n f \in \mathbb{P}_{n-1}(\Omega)$ of f consists in

$$\mathcal{F}_n f := \sum_{j=1}^{N_n} h\left(\frac{\deg p_j}{n}\right) \langle f, p_j \rangle_M p_j. \quad (5)$$

It can be easily seen, in view of the definition of the filter, that if $p \in \mathbb{P}_{\lfloor n/2 \rfloor}^d(\Omega)$ then $\mathcal{F}_n p = p$. Next, in [12] the authors show that (distributed) filtered hyperinterpolation can reduce weak noise.

One of the potential difficulties in (5) is the evaluation of $\deg p_j$, $j = 1, \dots, N_n$. This is straightforward for the classical spherical harmonics basis on \mathbb{S}^2 , since it is a *triangular basis*, i.e. for $k = 0, \dots, d$, $j = k^2 + 1, \dots, (k+1)^2$, we have $\deg p_j = k$.

In the case of the orthonormal basis $\{p_j\}_{j=1, \dots, N_n}$ on a spherical polygon \mathcal{P} , one has to take into account that it is computed numerically as specified above, by means of QR factorisation, starting from the Vandermonde matrix defined by spherical harmonics. Anyway, since R^{-1} is an upper triangular non-singular matrix, then the so

determined orthonormal basis (p_1, \dots, p_{N_n}) of $\mathbb{P}_n^3(\mathcal{P})$ is also triangular and again for $k = 0, \dots, d$, $j = k^2 + 1, \dots, (k+1)^2$, we have that $\deg p_j = k$.

An alternative approach consists in *Lasso hyperinterpolation* [1] that denoises perturbed data and attempts to dismiss less relevant discrete Fourier coefficients.

To this purpose, let us define the *soft thresholding operator* as

$$\mathcal{S}_k(a) := \max(0, a - k) + \min(0, a + k),$$

where $k \geq 0$, that is

$$\mathcal{S}_k(a) = \begin{cases} a + k, & \text{if } a < -k, \\ 0, & \text{if } -k \leq a \leq k, \\ a - k, & \text{if } a > k. \end{cases}$$

and suppose that a discrete scalar product $\langle f, g \rangle_M$ is given by an M -point cubature rule of PI-type in Ω with algebraic degree of exactness $2n$.

Then the *Lasso hyperinterpolation* of f onto $\mathbb{P}_L(\Omega)$ is defined as

$$\mathcal{L}_L^\lambda f := \sum_{j=1}^{N_n} \mathcal{S}_{\lambda \mu_j}(\langle f, p_j \rangle_M) p_j. \quad (6)$$

where $\lambda > 0$ is the regularization parameter and $\{\mu_k\}_{k=1}^{N_n}$ is a set of positive penalty parameters.

By the definition of $\mathcal{S}_k(a)$, if $|\langle f, p_k \rangle_M| \leq \lambda \mu_k$ then $\mathcal{S}_{\lambda \mu_k}(\langle f, p_k \rangle_M) = 0$, so explaining how it tries to dismiss less relevant discrete Fourier coefficients, slightly modifying the remaining ones. Differently from the classical hyperinterpolation and filtered hyperinterpolation, the Lasso operator is not in general a projection to a certain polynomial space and is not invariant under a change of basis.

In [1] the authors have shown theoretically and numerically the effectiveness \mathcal{L}_n^λ in the case of noisy data, taking advantage of the connection between $\mathcal{L}_n^\lambda f$ and a certain ℓ_1 -regularized least squares problem.

In order to combine the features of filtered and Lasso hyperinterpolation, in [2] the authors introduced the so called *hybrid hyperinterpolation*.

Suppose that the discrete scalar product $\langle f, g \rangle_M$ is determined as above by an M -points quadrature rule of PI-type in Ω with algebraic degree of exactness $2n$. The *hybrid hyperinterpolation* of f onto $\mathbb{P}_n^d(\Omega)$ is defined as

$$\mathcal{H}_n^\lambda f := \sum_{j=1}^{N_n} h\left(\frac{\deg p_j}{n}\right) \mathcal{S}_{\lambda \mu_j}(\langle f, p_j \rangle_M) p_j, \quad \lambda > 0, \quad (7)$$

where $h(\cdot)$ is a filter function, $\{\mathcal{S}_{\lambda \mu_j}(\cdot)\}_{j=1}^{N_n}$ are soft thresholding operators in which $\mu_k > 0$, $k = 1, \dots, N_n$.

Similarly to the case of the Lasso hyperinterpolation, by means of a connection between $\mathcal{H}_n^\lambda f$ and a certain $\ell_2^2 - \ell_1$ regularized least squares problem, in [2, Thm. 4.2] it is shown how hybrid hyperinterpolation acts on noisy data, with advantages in term of sparsity of its polynomial coefficients.

In the numerical section we report some examples, in which we show the performance of the classical hyperinterpolation as well as a comparison in problems dealing with noisy data.

Remark 1 *In this section we have not mentioned for sake of brevity some relevant hyperinterpolation variants as Hard Thresholding [5] or Tikhonov regularized least squares approximation that continuously shrinks all hyperinterpolation coefficients without dismissing less relevant ones.*

Remark 2 *We observe that, though \mathcal{L}_n requires the availability of an algebraic cubature rule with degree of precision $ADE = 2n$, some recent papers are considering the case when instead we have that $ADE < 2n$ and how this choice affects the approximation quality (see, e.g., [3],[4]).*

3.1 Numerical experiments

In our first numerical examples, we consider as spherical polygon \mathcal{P} that obtained as course map of Australia (without taking into account its smaller islands, lakes and rivers), scaled in S_2 and as functions those $f_k, k = 1, \dots, 6$ defined above.

In Figure 6 we report an approximation of the relative error

$$\frac{\|f_k(X) - (\mathcal{L}_n f_k)(X)\|_\infty}{\|f_k(X)\|_\infty} \approx \frac{\|f_k - \mathcal{L}_n f_k\|_\infty}{\|f_k\|_\infty}$$

where $n = 1, \dots, 10$ and X is the set of 82413 nodes of the rule on \mathcal{P} , with ADE equal to 10.

As somehow expected, the quality of the approximation of f_2, f_5 and f_6 via hyperinterpolation is *inferior* to that of f_1, f_3 and f_4 . Furthermore, since $f_1 \in \mathbb{P}_6$, in exact arithmetic we have $\mathcal{L}_n f_1 \equiv f_1$ for $n \geq 6$, so explaining why we get in this case relative errors close to 10^{-15} .

Next we plot in Figure 7 an approximation in semilogarithmic scale of $\|\mathcal{L}_n\|_\infty$ for $n = 1, \dots, 10$, a quantity that as seen above is fundamental to determine, in view of (3), an upper bound of $\|f - \mathcal{L}_n\|_\infty$ w.r.t. the best approximation error $E_n(f, \mathcal{P})$, where $f \in C(\mathcal{P})$.

To this purpose, defining the reproducing kernel $K_n(x, y) = \sum_{i=1}^{N_n} p_i(x)p_i(y)$ and $g_i(x) = w_i K_n(x_i, x)$, it can be proven that

$$\|\mathcal{L}_n\|_\infty = \max_{x \in \mathcal{P}} \sum_{i=1}^M |g_i(x)| \approx \max_{x \in X} \sum_{i=1}^M |g_i(x)|$$

where X is a sufficiently dense set of points. In our tests, we have chosen again as X the set of 82413 nodes of the rule on \mathcal{P} , with ADE equal to 10. The results show that for $n \leq 10$, the operator norm $\|\mathcal{L}_n\|$ is relatively small and thus, by (3), the approximation error is not too large w.r.t. that of the best approximant $E_n(f, \mathcal{P})$.

We report that, when the cubature formula is available, the computation of the hyperinterpolation coefficients $\mathbf{c}^* = (c_k)_{k=1, \dots, N_n}$, for $n \leq 10$, requires from $5 \cdot 10^{-4}$ to 10^{-2} seconds.

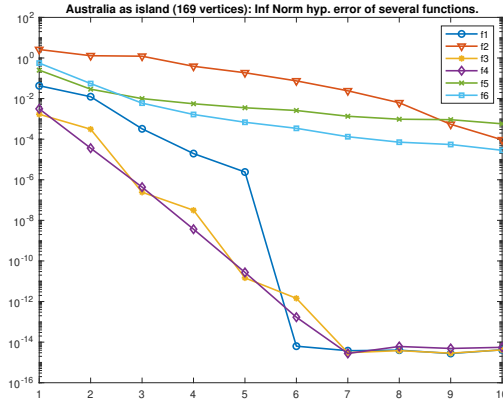


Figure 6: Inf-Norm hyperinterpolation relative error of several test functions over a coarse approximation of Australia.

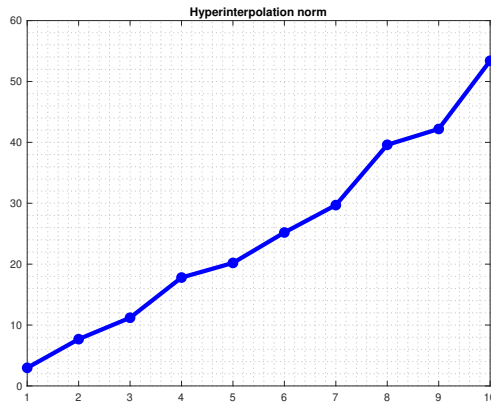


Figure 7: Approximation of the hyperinterpolation operator norm $\|\mathcal{L}_n\|$ when \mathcal{P} is a coarse approximation of Australia.

Next we intend to compare the proposed forms of hyperinterpolation, i.e. the classical one as well the filtered, the Lasso and the hybrid one on the case of noisy data in the spherical polygon \mathcal{P} adopted above.

As for filtered hyperinterpolation, following [2], we choose $h : [0, 1] \rightarrow [0, 1]$ defined as

$$h(x) = \begin{cases} 1, & x \in [0, \frac{1}{2}], \\ \sin^2(\pi x), & x \in [\frac{1}{2}, 1]. \end{cases}$$

	$\lambda \approx 0.011$	$\lambda \approx 0.0087$	$\lambda \approx 0.0073$	$\lambda \approx 0.0061$
<i>filtered</i>	0.070603	0.067005	0.069905	0.068639
<i>Lasso</i>	0.034094	0.035766	0.037304	0.03865
<i>hybrid</i>	0.033333	0.033969	0.034454	0.03513
<i>hyperint.</i>	0.079629	0.076223	0.079625	0.078205
<i>hybrid sparsity</i>	19	29	39	49

Table 2: Average approximation errors in the 2-norm and sparsity of hybrid hyperinterpolation coefficients of noisy versions of $f(x) = \exp((x^6) \cos(y + 2z))$, over a spherical polygon P that approximates the Australia, scaled on the unit-sphere \mathbb{S}_2 , via variants of hyperinterpolation of degree 10. The perturbation is obtained by the sum of impulse noise with $a = 0.25$ and of gaussian noise having standard deviation $\sigma = 0.25$.

In the experiments reported in Table 2, we consider noisy evaluations of

$$f(x, y, z) = \exp(x^6 \cdot \cos(y + 2z))$$

on the nodes $\{P_j\}_{j=1, \dots, 441}$ of a compressed cubature rule over \mathcal{P} with ADE equal to 20.

The perturbation is obtained by means of the sum of *Gaussian noise* $\mathcal{N}(0, \sigma^2)$ from a normal distribution with mean 0 and standard deviation σ , and of *impulse noise* $\mathcal{I}(a)$ that takes uniformly distributed random values in $[-a, a]$ with probability $1/2$. In these tests, we have set $a = 0.25$ and $\sigma = 0.25$.

Next, being p_{10} the chosen hyperinterpolant of degree 10 on the perturbed data $\{(P_j, f(P_j) + \varepsilon_j)\}_{j=1, \dots, 441}$, we estimate the errors $\|f - p_{10}\|_2$ via a discretization of the L_2 scalar product by means of a cubature rule with degree of precision 30. In Table 2 we report as result the average error over 10 trials.

As for the Lasso and hybrid parameters λ , we use some of the hyperinterpolant coefficients that are 20-th, 30-th, 40-th and 50-th in magnitude, while all μ_i are equal to 1.

In these tests the performance of Lasso and hybrid hyperinterpolation is superior to that of the classical and filtered hyperinterpolation. Observe that the latter does not depend on the choice of λ , so explaining why their results remain almost equal varying such parameter.

The last column shows the sparsity of the hybrid hyperinterpolation coefficients, i.e. the number of those that are non null, varying λ . As comparison, take into account that filtered and classical hyperinterpolation require 121 non null coefficients.

As final experiments, we report in Table 3, the results obtained as in the previous example but fixing λ and varying a and σ , i.e. the amount of noise. In this framework the chosen values of λ , each time obtained as the 20-th hyperinterpolation coefficient in magnitude, vary in the interval $[0.0114, 0.0150]$.

We observe the advantage of using filtered or classic hyperinterpolation in case of mild noise while it is clear the counterpart when the perturbation is more significative.

We conclude saying that all the Matlab codes for hyperinterpolation on spherical polygons used in this work are available as open-source software at [17].

	$a = \sigma = 0.025$	$a = \sigma = 0.05$	$a = \sigma = 0.1$	$a = \sigma = 0.3$
<i>filtered</i>	0.00678	0.0137	0.0276	0.0844
<i>Lasso</i>	0.0124	0.0151	0.0200	0.0391
<i>hybrid</i>	0.0124	0.0150	0.0198	0.0376
<i>hyperint.</i>	0.0076	0.0157	0.0313	0.0964
<i>hybrid sparsity</i>	19	19	19	19

Table 3: Average approximation errors in the 2-norm and sparsity of hybrid hyperinterpolation coefficients of noisy versions of $f(x) = \exp((x^6) \cos(y + 2z))$, over a spherical polygon P that approximates the Australia, scaled on the unit-sphere \mathbb{S}_2 , via variants of hyperinterpolation of degree 10. The perturbation is obtained by the sum of impulse noise with several values of a and of gaussian noise having standard deviation σ , taking as λ the 10-th Fourier coefficient in magnitude of hyperinterpolation.

References

- [1] C. An and H.-N. Wu, *Lasso hyperinterpolation over general regions*, SIAM J. Sci. Comput., 43 (2021).
- [2] C. An, J.-S. Ran and A. Sommariva, *hybrid hyperinterpolation over general regions*, submitted, <https://arxiv.org/abs/2305.05863>.
- [3] C. An and H.-N. Wu, *On the quadrature exactness in hyperinterpolation*, BIT Numer. Math., 62 (2022), pp. 1899–1919.
- [4] C. An and H.-N. Wu, *Bypassing the quadrature exactness assumption of hyperinterpolation on the sphere*, Journal of Complexity Volume 80, February 2024, 101789.
- [5] C. An, J.-S. Ran, *Hard thresholding hyperinterpolation over general regions*, <https://arxiv.org/abs/220914634>.
- [6] K. Atkinson, *Numerical integration on the sphere*, J. Austral. Math. Soc. Ser. B 23 (1981/82), pp. 332–347.
- [7] Chebfun, numerical computing with functions, <http://www.chebfun.org>.
- [8] M. Dessoie, F. Marcuzzi and M. Vianello, *Accelerating the Lawson-Hanson NNLS solver for large-scale Tchakaloff regression designs*, Dolomites Res. Notes Approx. DRNA 13 (2020), pp. 20–29.
- [9] G. Da Fies, A. Sommariva and M. Vianello, *Algebraic cubature by linear blending of elliptical arcs*, Appl. Numer. Math. 74 (2013), pp. 49–61.
- [10] G. Da Fies, A. Sommariva and M. Vianello, *Subperiodic Trigonometric Hyperinterpolation*, "Festschrift for the 80th Birthday of Ian Sloan" (invited paper), J. Dick, F.Y. Kuo, H. Wozniakowski Eds., Springer, 2018, pp. 283–304.

- [11] C.L. Lawson, R.J. Hanson, *Solving Least Squares Problems*, Classics in Applied Mathematics 15, SIAM, Philadelphia, 1995.
- [12] S-B. Lin, Y.G. Wang, D.-X. Zhou, *Distributed filtered hyperinterpolation for noisy data on the sphere*, SIAM J. Numer. Anal. 2 (2021), pp. 634–659.
- [13] J. O’Rourke, *Computational Geometry Column 51*, ACM SIGACT News, September 2008, Vol. 40. No 3.
- [14] M. Slawski, Nonnegative least squares: comparison of algorithms. Paper and codes are available online at: <https://sites.google.com/site/slawskimartin/code>.
- [15] I.H. Sloan, *Interpolation and hyperinterpolation over general regions*, J. Approx. Theory 83 (1995), pp. 238–254.
- [16] I.H. Sloan and R.S. Womersley, *filtered hyperinterpolation: a constructive polynomial approximation on the sphere*, Int. J. Geomath. 3 (2012), pp. 95–117.
- [17] A. Sommariva, *Matlab codes for cubature and hyperinterpolation on spherical polygons*, https://github.com/alvisesommariva/CUB_SPHPOLY.
- [18] A. Sommariva and M. Vianello, *Compression of multivariate discrete measures and applications*, Numer. Funct. Anal. Optim. 20 (2015), pp. 1198–1223.
- [19] A. Sommariva and M. Vianello, *Numerical hyperinterpolation over nonstandard planar regions*, Mathematics and Computers in Simulation, Volume 141, 10 (2017), pp. 110–120.
- [20] A. Sommariva and M. Vianello, *Near-algebraic Tchakaloff-like cubature on spherical triangles*, Appl. Math. Lett. (120) 2021, pp. 107282.
- [21] A. Sommariva and M. Vianello, *Numerical hyperinterpolation over spherical triangles*, Math. Comp. Simul. (190) 2021, pp. 15-22.
- [22] M. Vianello, *dCATCH: numerical package for d-variate polynomial fitting (computes d-variate compressed near G-optimal designs on discrete sets)*, <https://www.math.unipd.it/~marcov/dCATCH.html>.